Behavioral Modeling of (Coupled) Harmonic Oscillators

Piet Vanassche, Georges Gielen and Willy Sansen
Katholieke Universiteit Leuven - ESAT/MICAS
Kasteelpark Arenberg 10, B-3001 Leuven, Belgium
piet.vanassche@esat.kuleuven.ac.be

ABSTRACT

A new approach is presented for the construction of behavioral models for harmonic oscillators and sets of coupled harmonic oscillators. The models can be used for system-level simulations and trade-off analysis. Besides the steady-state behavior, the model also takes the transient behavior of the oscillation amplitudes and phase differences into account. This behavior is modeled using a set of linear differential equations. Their extraction from a netlist description is based upon the ideas of perturbation analysis and stochastic averaging. The modeling equations are valid in the neighbourhood of the oscillator's steady-state operating point and can be evaluated at very low computational cost. Another major advantage of the approach is that it explicitely separates the fast-varying steady-state behavior and the slow-varying transient behavior. This allows for straightforward application of multi-rate simulation techniques, greatly boosting simulation speeds. The technique is illustrated for a quadrature oscillator.

Categories and Subject Descriptors

G.1.7 [**Mathematics of Computing**]: Ordinary Differential Equations; I.6.5 [**Computing Methodologies**]: Model Development—*modeling methodologies*

General Terms

Algorithms, Theory

Keywords

Averaging, Behavioral modeling, Coupled harmonic oscillators, Perturbation theory

1. INTRODUCTION

Compact behavioral models of system-level building blocks, like filters, mixers and oscillators, are needed for several reasons. From a bottom-up point of view, they allow for efficient system-level verification. From a top-down point of view, they can be used for trade-off analysis and specification translation. They also assist in understanding the interactions that take place between the building block and its surroundings. To this account, behavioral models should both be accurate and allow efficient evaluation.

This paper presents an approach for behavioral modeling of harmonic oscillators and sets of coupled harmonic oscillators. The term harmonic oscillator means that the oscillation principle is based upon energy resonating between a magnetic field (an inductor) and an electric field (a capacitor). Harmonic oscillators are used in many RF-applications [12] because of their good linearity and phase noise performance. Coupled harmonic oscillators occur for example in zero- and low-IF receiver systems where one needs both an in-phase and a quadrature oscillation [2]. The modeling approach presented in this paper allows to capture the steady-state, transient and noise behavior of this type of oscillators.

When looking at the behavioral oscillator models published in litterature, oscillators are often treated as simple phase-integrating elements [3, 10]. In these models, amplitudes and phase differences are treated as constants. They neglect all of the oscillator's transients. Also, there is no systematic way of incorporating the influence of noise into the behavioral modeling equations. In recent years, more systematic modeling approaches have emerged as people investigated the oscillator's phase noise behavior [4, 6, 7]. That work, however, has only been concerned with the behavior of the (common-mode) phase θ. Although [7] also discusses amplitude variations, the behavior of the phase differences of coupled oscillators is never adressed. Another interesting approach towards oscillator analysis was presented in [11], where one uses a multivariate method to separate the fast-varying, steady-state, time constants and the slow-varying, transient, time constants. That work, however, only addresses the simulation issue and not the extraction of a compact behavioral model.

The work presented in this paper builds upon the multi-variate idea to generate separate models describing the fast-varying, steady-state, and the slow-varying, transient, behavior. More precisely, it is shown that the behavior of a set of coupled harmonic oscillators can be modeled as

$$v_{osc}(t) = A_k(t)\cos\left(\omega_{osc}t + \theta(t) + \Delta\phi_k(t)\right) \qquad (1)$$

where the amplitudes $A_k(t)$, the common-mode phase $\theta(t)$ and the phase differences $\Delta\phi_k(t)$ –measured with respect to the phase of some reference oscillator– are slow-varying compared to the oscillation time constant. In a first-order approximation, these slow-varying processes are shown to be governed by a system of linear ordinary differential equations (ODEs). This provides a very compact model which is evaluated at low computational cost. The model extraction procedure builds upon the ideas of perturbation theory [8] and averaging [1, 8, 9, 13]. It is found to be especially well suited for oscillators with a moderate to high Q-factor of the

DAC 2002, June 10-14, 2002, New Orleans, Louisiana, USA.

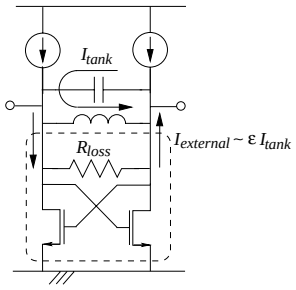

Figure 1: Decomposition of a harmonic oscillator into a lossless resonance tank and external sources changing the tank energy. Inductor and capacitor losses are considered to be part of these external sources and are modeled using the resistor R_{loss}.

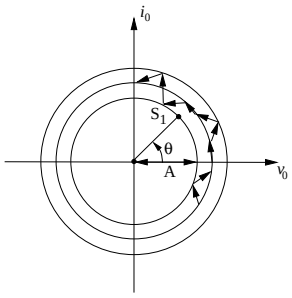

Figure 2: For a single harmonic oscillator, each solution of the *unperturbed* system is characterized by an amplitude A and an initial phase θ. Such a solution can hence be represented as a single point in a 2-dimensional space. The transient behavior of the *perturbed* system can then be considered as the oscillator "slipping" from one solution of the unperturbed system to another one as indicated by the arrows.

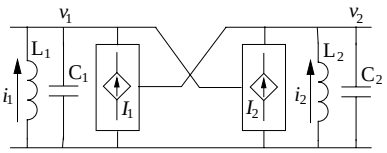

Figure 3: A system of two coupled harmonic oscillators can be decomposed into two independent resonance tanks which are coupled through voltage-controlled current sources.

resonance tank. Current testing has shown the approach to work for $Q \geq 5$. By separating fast-varying and slow-varying behavior, it allows for straightforward application of multi-rate simulation techniques, greatly boosting simulation speeds.

The remainder of this paper is organized as follows. Section 2 outlines the general ideas upon which the modeling approach is founded. In section 3, perturbation analysis of (coupled) harmonic oscillators allows us to construct a set of ODEs governing the behavior of the oscillation amplitudes and phase differences. In section 4, we apply the averaging technique to separate the fast-varying, steady-state, and slow-varying, transient, time constants. In section 5, we linearize the equations in the neighbourhood of the oscillator's operating point. Section 6, discusses how to extract the behavioral model from a given netlist, while section 7 experimentally demonstrates our approach on a harmonic quadrature oscillator. Finally, conclusions are drawn in section 8.

2. FUNDAMENTAL CONCEPTS

Separating the steady-state and transient behavior of a harmonic oscillator basically comes down to decomposing the oscillator circuit into a set of lossless resonance tanks and a set of "external" sources modifying the energy contained in the tanks. This decomposition is illustrated in Fig. 1 for a single harmonic oscillator. The part encircled by the dashed line is the collection of sources modifying the resonance tank energy. These sources also include inductor and capacitor losses which can be modeled using a parallel resistor R_{loss}.

In practical realizations, the energy injections by the external sources are kept as limited as possible. Typically, larger sources generate more noise, contributing for example to bad phase noise behavior. In most cases, the active elements are designed to be just large enough to compensate for the tank losses due to R_{loss}. This design implies that the currents $I_{external}$ injected by the external sources into the resonance tank are an order of magnitude smaller than the current already circulating within the tank, or

$$I_{external} \sim \epsilon I_{tank} \tag{2}$$

with $\epsilon \ll 1$.

When left unperturbed, the resonant tank voltages and currents will settle onto a circular orbit in phase space. Such a solution of the unperturbed system is completely characterized by its amplitude and initial phase, or equivalently by the initial voltage v_0 over the capacitor and the initial current i_0 through the inductor. It can hence be represented as a single point in a two-dimensional space, for example S_1 in Fig. 2. Injection of the currents $I_{external}$ will however disturb the energy in the resonance tank, causing changes in its oscillation amplitude and phase. It is hence the interaction between the resonance tank and the external sources which causes the oscillator's transient behavior. This transient behavior can be interpreted as the oscillator slipping from one solution of the unperturbed system to another. This behavior is illustrated in Fig. 2. Since the energy injected per oscillation period T is small, these transient changes will be slow compared to the period of oscillation. More precisely, these changes occur on a time scale T/ϵ, with ϵ determined by equation (2).

From the discussion above, it follows that the behavior of the oscillator is completely determined by the characteristics of the unperturbed system, the fast-oscillating resonance tank, and the equations characterizing the slow-varying behavior of its amplitude and phase. As will be discussed in section 4, the ODEs governing this slow-varying behavior can be separated from the fast steady-state oscillation using the averaging technique. This technique relies on the assumption that, over a single oscillation period, amplitudes and phases can be considered constant. This yields a model for the transient behavior that can be solved on a time scale T/ϵ.

The discussion above can easily be extended to a system of K coupled harmonic oscillators. In this case, the system is separated into K independent resonance tanks which are mutually coupled through controlled current sources. Fig. 3 illustrates this for $K = 2$. This template will serve as a starting point for our analysis in the next sections. In section 6, we will discuss how to map a given circuit topology on this template. Note that it is also possible to deal with other types of resonance tanks, like capacitor-inductor series connections. Adjustments are straightforward but are not discussed within this text.

3. PERTURBATION ANALYSIS

A system of K coupled harmonic oscillators, as depicted in Fig. 3

for $K = 2$, is described by the normalized system of equations

$$\begin{aligned} \frac{d\bar{i}_k}{d\bar{t}} &= \bar{v}_k + \epsilon\delta_k \frac{d\bar{i}_k}{d\bar{t}} \\ \frac{d\bar{v}_k}{d\bar{t}} &= -\bar{i}_k - \epsilon \bar{I}_k\left(\bar{v}_1, \frac{d\bar{v}_1}{dt}, \bar{v}_2, \frac{d\bar{v}_2}{dt}, \ldots, \bar{t}\right) + \epsilon\delta_k \frac{d\bar{v}_k}{d\bar{t}} \end{aligned} \tag{3}$$

for $k = 1, \ldots, K$. The normalized quantities are related to the actual voltages and currents through $\bar{v}_k = \frac{v_k}{V_k}$, $\bar{i}_k = \frac{i_k}{\omega_{0,k} C_k V_k}$, $\bar{I}_k\left(\bar{v}_1, \frac{d\bar{v}_1}{dt}, \ldots, t\right) = \frac{I_k(v_1, \frac{dv_1}{dt}, \ldots, t)}{I_{k,max}}$ and $\bar{t} = \omega_0 t$. Furthermore,

$$\epsilon = \frac{I_{k,max}}{\omega_{0,k} C_k V_k} \tag{4}$$

Here, $\omega_{0,k} = 1/\sqrt{L_k C_k} = \omega_0 (1 + \epsilon\delta_k)$ is the resonance frequency of the k-th tank. We assume these resonance frequencies to be clustered around their geometric mean $\omega_0 = \left(\prod_k \omega_{0,k}\right)^{1/k}$, or $\delta_k \leq 1$. Furthermore, V_k is an estimate for the magnitude of the voltage swing over the capacitor C_k. It should be chosen such that (4) yields the same ϵ for all k. $I_{k,max}$ is a measure for the maximum current delivered by the active elements. Using vector notation, the system (3) looks like

$$\frac{d\mathbf{x}}{dt} = \mathbf{L}\mathbf{x} + \epsilon \mathbf{g}\left(\mathbf{x}, \frac{d\mathbf{x}}{dt}, t\right) \tag{5}$$

where $\mathbf{x}(t) = \begin{bmatrix} \bar{i}_1(t) & \bar{v}_1(t) & \bar{i}_2(t) & \bar{v}_2(t) & \cdots \end{bmatrix}^T \in \mathbb{R} \to \mathbb{R}^{2K}$, $\mathbf{L} \in \mathbb{R}^{2K \times 2K}$ and $\mathbf{g}(\cdot,\cdot,\cdot) \in \mathbb{R}^{2K} \times \mathbb{R}^{2K} \times \mathbb{R} \to \mathbb{R}^{2K}$. The nature of the oscillation is characterized by the parameter ϵ, defined by equation (4). If $\epsilon \ll 1$, the oscillation is essentially one where energy resonates between an electric and a magnetic field, with the active elements only weakly involved to compensate for dissipative losses. If $\epsilon \gg 1$, the active elements dominate the oscillating behavior, and we get a relaxation type oscillator. For harmonic oscillators with a sufficiently high Q-factor, i.e. the type of oscillators being considered in this text, it holds that $\epsilon \sim \frac{1}{Q} \ll 1$.

In constructing a compact behavioral model equivalent to the original system (5), we proceed along the same lines of reasoning as outlined in [1, 9]. For $\epsilon \to 0$, i.e. for the unperturbed oscillator, (3) is solved by

$$\bar{i}_k(t) = A_k \sin(t + \theta_k) \tag{6}$$

$$\bar{v}_k(t) = A_k \cos(t + \theta_k) \tag{7}$$

with $\bar{i}_k(t)$ and $\bar{v}_k(t)$ 2π-periodic processes. In vector notation this becomes

$$\mathbf{x}(t) = \mathbf{x}_s(t; \mathbf{p}) \tag{8}$$

where $\mathbf{x}_s \in \mathbb{R} \times \mathbb{R}^{2K} \to \mathbb{R}^{2K}$ and

$$\mathbf{p} = \begin{bmatrix} A_1 & \cdots & A_K & \theta_1 & \cdots & \theta_K \end{bmatrix}^T \in \mathbb{R}^{2K} \tag{9}$$

For unperturbed oscillators, amplitudes and phases are determined by the initial conditions and remain constant with respect to time, i.e. they can be considered as constants of motion characterizing a particular periodic solution.

Under the influence of weak perturbations, i.e. for $\epsilon \ll 1$, the oscillation amplitudes and phases will no longer remain constant, but will slowly change values with time. This is the "slipping" behavior as outlined in section 2 and illustrated in Fig. 2. This implies that the solution of the perturbed system can be modeled as

$$\mathbf{x}(t) = \mathbf{x}_s(t; \mathbf{p}(t)) \tag{10}$$

where the vector $\mathbf{p}(t)$ is no longer a constant, but is evolving with time. The equations governing this "slipping" behavior are found by substituting the signal model (10) into the ODEs (5). Up to first order in ϵ, this yields

$$\frac{d\mathbf{p}}{dt} = \epsilon \mathbf{h}_p(t; \mathbf{p}) \tag{11}$$

with $\mathbf{h}_p(t; \mathbf{p}) \in \mathbb{R} \times \mathbb{R}^{2K} \to \mathbb{R}^{2K}$ determined by

$$\mathbf{h}_p(t; \mathbf{p}) = \frac{\partial \mathbf{x}_s}{\partial \mathbf{p}}(t; \mathbf{p})^{-1} \mathbf{g}\left(\mathbf{x}_s(t; \mathbf{p}), \frac{\partial \mathbf{x}_s}{\partial t}(t; \mathbf{p}), t\right) \tag{12}$$

As the Jacobian matrix $\frac{\partial \mathbf{x}_s}{\partial \mathbf{p}}(t; \mathbf{p})$ in equation (12) is concerned, it is easy to show that it has a block-diagonal structure with

$$\mathbf{J}_k(t; \mathbf{p}) = \begin{bmatrix} \sin(t + \theta_k) & A_k \cos(t + \theta_k) \\ \cos(t + \theta_k) & -A_k \sin(t + \theta_k) \end{bmatrix} \tag{13}$$

being the (block)-diagonal elements. Its inverse is also block-diagonal with the diagonal elements equal to

$$\mathbf{J}_k(t; \mathbf{p})^{-1} = \frac{1}{A_k} \begin{bmatrix} A_k \sin(t + \theta_k) & A_k \cos(t + \theta_k) \\ \cos(t + \theta_k) & -\sin(t + \theta_k) \end{bmatrix} \tag{14}$$

In a final step, we change variables, reformulating (12) in terms of one common-mode phase θ and the phase differences $\Delta\phi$ between the oscillators. The reason for this reformulation lies in the fact that, for most practical applications, the phase differences between the oscillators are of greater interest than their absolute values. These phase differences are often required to converge to some fixed value, a property we will use later on in our model extraction procedure. Introducing the vector

$$\mathbf{q} = \begin{bmatrix} A_1 & \cdots & A_K & \Delta\phi_2 & \cdots & \Delta\phi_K & \theta \end{bmatrix}^T \tag{15}$$

$$= \mathbf{T}_q^{-1} \mathbf{p} \tag{16}$$

with $\theta = \theta_1$, $\Delta\phi_k = \theta_k - \theta_1$ and $\mathbf{T}_q \in \mathbb{R}^{2K \times 2K}$, the ODE (12) can be recast into

$$\frac{d\mathbf{q}}{dt} = \epsilon \mathbf{h}_q(t; \mathbf{q}) \tag{17}$$

where

$$\mathbf{h}_q(t; \mathbf{q}) = \mathbf{T}_q \left[\frac{\partial \mathbf{x}_s}{\partial \mathbf{p}}(t; \mathbf{T}_q^{-1}\mathbf{q})\right]^{-1} \mathbf{g}\left(\mathbf{x}_s, \frac{\partial \mathbf{x}_s}{\partial t}, t\right) \tag{18}$$

Here, $\mathbf{x}_s$ stands short for $\mathbf{x}_s\left(t; \mathbf{T}_q^{-1}\mathbf{q}\right)$. In what follows, (17) serves as a starting point for extraction of a compact behavioral model for the dynamic behavior of a set of coupled harmonic oscillators.

4. AVERAGING

Equation (17) learns that the transient changes in $\mathbf{q}(t)$ occur on a time scale t/ϵ. This means that, over one oscillation period, $\mathbf{q}(t)$ can be considered a constant. This observation is the foundation of the averaging technique in [1, 9], where it was first discussed for deterministic systems, and [5], where it is extended to include noisy inputs. In what follows, we use the results obtained in [5] to extract a set of equations describing the oscillator's transient behavior.

In order to apply the averaging technique properly, we need to separate the deterministic and stochastic processes at the oscillator input. To this account, we assume that the perturbation part in the right-hand side of equation (5) can be written as

$$\mathbf{g}\left(\mathbf{x}, \frac{d\mathbf{x}}{dt}, t\right) = \mathbf{g}_d\left(\mathbf{x}, \frac{d\mathbf{x}}{dt}, \mathbf{u}\right) + \mathbf{G}_n\left(\mathbf{x}, \frac{d\mathbf{x}}{dt}, \mathbf{u}\right)\mathbf{n}(t) \tag{19}$$

Here, $\mathbf{u}(t) \in \mathbb{R} \to \mathbb{R}^U$ represents a vector of slow-varying, deterministic inputs and $\mathbf{n}(t) \in \mathbb{R} \to \mathbb{R}^N$ is a vector of uncorrelated,

standard (normalized) white noise sources. The assumption of the deterministic inputs $\mathbf{u}(t)$ being slow-varying, i.e. varying on a time scale t/ϵ, seems justified by the fact that these inputs are typically control signals which should never vary faster than the transients of the oscillator they try to control. Combining the equations (18) and (19), the right-hand side $\mathbf{h}_q(t;\mathbf{q})$ in equation (17) can be split into a determistic and a stochastic component, or

$$\mathbf{h}_q(t;\mathbf{q}) = \mathbf{h}_d(t;\mathbf{q},\mathbf{u}) + \mathbf{H}_n(t;\mathbf{q},\mathbf{u})\,\mathbf{n}(t) \tag{20}$$

where both $\mathbf{h}_d(t,\cdot,\cdot) \in \cdot \to \mathbb{R}^{2K}$ and $\mathbf{H}_n(t;\cdot) \in \cdot \to \mathbb{R}^{2K\times N}$ are 2π-periodic in t. Using furthermore the fact that the last component of the vector $\mathbf{q}$, i.e. the reference phase θ, will always appear in combination with the time variable t as $t+\theta$, and with $\mathbf{q}_1$ being defined by $\mathbf{q} = \begin{bmatrix} \mathbf{q}_1^T & \theta \end{bmatrix}^T$, The ODE (17) is transformed into

$$\frac{d}{dt}\begin{bmatrix} \mathbf{q}_1 \\ \theta \end{bmatrix} = \epsilon\left(\mathbf{h}_d(t+\theta;\mathbf{q}_1,\mathbf{u}) + \mathbf{H}_n(t+\theta;\mathbf{q}_1,\mathbf{u})\,\mathbf{n}(t)\right) \tag{21}$$

which, because of the noise terms, is a system of stochastic differential equations.

Using the averaging principle [1, 5], it can be shown that for ϵ being small, the solution of (21) converges to that of the "averaged" equation

$$\frac{d}{dt}\begin{bmatrix} \mathbf{q}_1 \\ \theta \end{bmatrix} = \epsilon\left(\overline{\mathbf{h}}_d(\mathbf{q}_1,\mathbf{u}) + \overline{\mathbf{H}}_n(\mathbf{q}_1,\mathbf{u})\,\overline{\mathbf{n}}(t)\right) \tag{22}$$

with

$$\overline{\mathbf{h}}_d(\mathbf{q}_1,\mathbf{u}) = \frac{1}{2\pi}\int_0^{2\pi} \mathbf{h}_d(t;\mathbf{q}_1,\mathbf{u})\,dt \tag{23}$$

and

$$\overline{\mathbf{H}}_n(\mathbf{q}_1,\mathbf{u}) = \sqrt{\frac{1}{2\pi}\int_0^{2\pi} \mathbf{H}_n(t;\mathbf{q}_1,\mathbf{u})\,\mathbf{H}_n(t;\mathbf{q}_1,\mathbf{u})^T\,dt} \tag{24}$$

In equation (22), $\overline{\mathbf{n}}(t) \in \mathbb{R}\times\mathbb{R}^{\overline{N}}$ again is a vector of uncorrelated, standard white noise processes.

5. LINEARIZATION

With its right-hand side independent of θ, the system (22) can be separated into two subsystems, one modeling the transient behavior of the vector $\mathbf{q}_1$, i.e. the amplitudes A_k and the phase differences $\Delta\phi_k$, and another one modeling the behavior of the common phase θ. These systems are given by

$$\frac{d\mathbf{q}_1}{dt} = \epsilon\left(\overline{\mathbf{h}}_{d,1}(\mathbf{q}_1,\mathbf{u}) + \overline{\mathbf{H}}_{n,1}(\mathbf{q}_1,\mathbf{u})\,\overline{\mathbf{n}}(t)\right) \tag{25}$$

$$\frac{d\theta}{dt} = \epsilon\left(\overline{\mathbf{h}}_{d,2}(\mathbf{q}_1,\mathbf{u}) + \overline{\mathbf{H}}_{n,2}(\mathbf{q}_1,\mathbf{u})\,\overline{\mathbf{n}}(t)\right) \tag{26}$$

where $\overline{\mathbf{h}}_{d,1}$, $\overline{\mathbf{h}}_{d,2}$ are the first $2k-1$ rows, respectively the last row of the vector $\overline{\mathbf{h}}_d$ and $\overline{\mathbf{H}}_{n,1}$, $\overline{\mathbf{H}}_{n,2}$ are likewise extracted from $\overline{\mathbf{H}}_n$.

For a properly designed, stable oscillator and for a constant input $\mathbf{u}(t) = \mathbf{u}_{op}$ (the nominal control voltage of a VCO), the solution of the system (25) converges to the neighbourhood of a fixed point $\mathbf{q}_{1,op}$ determined by

$$\overline{\mathbf{h}}_{d,1}(\mathbf{q}_{1,op},\mathbf{u}_{op}) = 0 \tag{27}$$

A good approximation of the oscillator's transient behavior in the neighbourhood of such a fixed point is found by linearizing (25) and (26) around the desired operating point $\mathbf{q}_{1,op}$. With $\mathbf{q}_1(t) = \mathbf{q}_{1,op} + \Delta\mathbf{q}_1(t)$ and $\mathbf{u}(t) = \mathbf{u}_{op} + \Delta\mathbf{u}(t)$, this yields

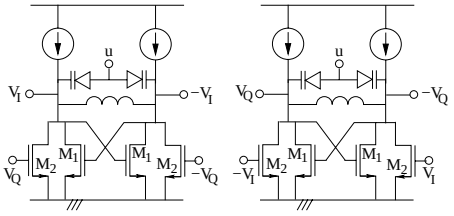

Figure 4: Basic quadrature oscillator topology used to illustrate the numerical methods involved in extracting the behavioral model.

$$\frac{d\Delta\mathbf{q}_1}{dt} = \mathbf{A}_1\Delta\mathbf{q}_1 + \mathbf{B}_{u,1}\Delta\mathbf{u}(t) + \mathbf{B}_{n,1}\overline{\mathbf{n}}(t) \tag{28}$$

with $\mathbf{A}_1 = \epsilon\frac{\partial\overline{\mathbf{h}}_{d,1}}{\partial\mathbf{q}_1}\left(\mathbf{q}_{1,op},\mathbf{u}_{op}\right) \in \mathbb{R}^{(2K-1)\times(2K-1)}$, etc. Note that for the operating point $\left(\mathbf{q}_{1,op},\mathbf{u}_{op}\right)$ to be stable, all eigenvalues of the matrix $\mathbf{A}_1$ should be located in the left half plane.

In the neighbourhood of the operating point $\left(\mathbf{q}_{1,op},\mathbf{u}_{op}\right)$, the behavior of the common phase θ is likewise determined by

$$\frac{d\theta}{dt}(t) = \Delta\omega_0 + \mathbf{A}_2\Delta\mathbf{q}_1(t) + \mathbf{B}_{u,2}\Delta\mathbf{u}(t) + \mathbf{B}_{n,2}\overline{\mathbf{n}}(t) \tag{29}$$

where $\Delta\omega_0 = \epsilon\overline{\mathbf{h}}_{d,2}(\mathbf{q}_{1,op},\mathbf{u}_{op}) \in \mathbb{R}$, $\mathbf{A}_2 = \epsilon\frac{\partial\overline{\mathbf{h}}_{d,2}}{\partial\mathbf{q}_1}(\mathbf{q}_{1,op},\mathbf{u}_{op}) \in \mathbb{R}^{1\times(2K-1)}$, etc. For a free-running oscillator in steady-state regime, i.e. with $\Delta\mathbf{q}_1(t) = 0$ and $\Delta\mathbf{u}(t) = 0$, equation (29) implies that

$$\theta(t) = \Delta\omega_0 t + \sqrt{\mathbf{B}_{n,2}\mathbf{B}_{n,2}^T}B(t) \tag{30}$$

with $B(t)$ being a standard Brownian motion. In (30), $\Delta\omega_0$ represents the deviation of the actual oscillation frequency from the natural frequency of the resonance tank. The second term is the phase-noise component as discussed in [4].

Equations (28)-(29) specify a behavioral model that completely characterizes the transient behavior of a set of coupled harmonic oscillators in the neighbourhood of the operating point $\left(\mathbf{q}_{1,op},\mathbf{u}_{op}\right)$. Once $\mathbf{A}_1$, $\mathbf{A}_2$, $\mathbf{B}_{u,1}$, $\mathbf{B}_{u,2}$, $\mathbf{B}_{n,1}$, $\mathbf{B}_{n,2}$ and $\Delta\omega_0$ have been determined, something which needs to be done only once, evaluation of the model comes at a minimal computational cost. This is particularly interesting when long (or repetitive) simulations need to be performed.

6. NUMERICAL COMPUTATIONS

In extracting the model equations (28)-(29) from a given circuit-level description, we need to map the circuit topology on the template of Fig. 3 (where it is illustrated for $K = 2$). Here, the current sources I_k should include all energy dissipating elements, also the ones arising from capacitor and inductor losses. Furthermore, we must find a way to evaluate the functions $\overline{\mathbf{h}}_d(\mathbf{q}_1,\mathbf{u})$ and $\overline{\mathbf{H}}_n(\mathbf{q}_1,\mathbf{u})$. In what follows, we outline the computational procedures for the example of the harmonic quadrature oscillator shown in Fig. 4. Adjusting this approach for other types of (coupled) harmonic oscillators is straightforward.

The characteristics of the oscillator resonance tanks, more specifically the effective capacitance and inductance values C_k and L_k, are determined by fitting the frequency characteristic of the admittance $G(j\omega)$ of an RLC tank to the one measured using the simulation setup shown in Fig. 5. This setup is simply a single oscilla-

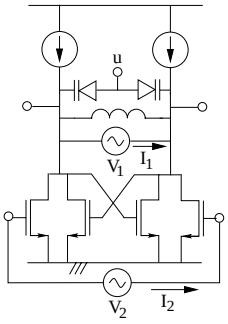

Figure 5: Measurement setup used to extract the resonance tank characteristic and the currents $I_k\left(v_1, \frac{dv_1}{dt}, v_2, \frac{dv_2}{dt}, \ldots, t\right)$ exchanged between the resonance tank and the remainder of the circuit.

tor section, where a given in-phase and quadrature voltage are enforced using the voltage sources V_1 and V_2. To obtain the circuit's $G(j\omega)$, we use the results of an AC analysis in the neighbourhood of $V_1 = V_2 = 0$. This involves applying

$$V_1(t) = \Delta v \cos(\omega t) \quad (31)$$

$$V_2(t) = 0 \quad (32)$$

with Δv a sufficiently small voltage. Measuring the (steady-state) current $I_1(t)$ through the voltage source V_1 allows us to compute $G(j\omega) = I_1/V_1$. The fitting is performed for frequencies ω in the neighbourhood of the resonance frequency ω_0, detemined by

$$\omega_0 = \arg\min_{\omega} |G(j\omega)| \quad (33)$$

All of this needs to be done for the external (control) inputs set to their nominal DC value, or $\mathbf{u} = \mathbf{u}_{op}$. Note that use of the setup in Fig. 5 implies that the transistor capacitances are taken into account as part of the effective tank capacitance C_k.

Computation of $\overline{\mathbf{h}}_d(\mathbf{q}_1, \mathbf{u})$ and $\overline{\mathbf{H}}_n(\mathbf{q}_1, \mathbf{u})$, for a given set of values for $\mathbf{q}_1$ and $\mathbf{u}$, basically requires evaluation of the currents I_k. Evaluating, for example, $I_1\left(v_1, \frac{dv_1}{dt}, v_2, \frac{dv_2}{dt}, \ldots, t\right)$ is done by applying

$$V_1(t) = A_1 \cos(\omega_0 t + \theta) \quad (34)$$

$$V_2(t) = A_2 \cos(\omega_0 t + \theta + \Delta\phi_2) \quad (35)$$

in the measurement setup of Fig. 5. $I_1\left(v_1, \frac{dv_1}{dt}, v_2, \frac{dv_2}{dt}, \ldots, t\right)$ then equals the (steady-state) current $I_1(t)$ flowing through the voltage source V_1. In computing this current I_1, the (slow-varying) input signals $\mathbf{u}(t)$ should be kept at a constant value. The deterministic component $\overline{\mathbf{h}}_d(\mathbf{q}_1, \mathbf{u})$ is separated from the stochastic component $\overline{\mathbf{H}}_n(\mathbf{q}_1)$ by first setting all noise sources to zero, which leaves only the deterministic component to be measured. The stochastic component then follows from (time-varying) linearization in the neighbourhood of the "large-signal" deterministic component.

7. EXPERIMENTAL RESULTS

The model extraction procedure was implemented in Matlab for the harmonic quadrature oscillator shown in Fig. 4. We compared both the behavioral model's steady-state and transient behavior with the results obtained from SPICE-like simulation algorithms. In Matlab, transistor modeling was done based upon the MOST level-1 current equations, as no link between Matlab and more sophisticated SPICE transistor models was available. All computations were done starting from the normalized system of equations (3). Extraction of the behavioral model takes a few minutes on a Sun Ultra30.

	$\gamma = 0.5, m = 0.3$		$\gamma = 0.5, m = 0.5$	
	Original	Model	Original	Model
A_1	2.51	2.51	2.62	2.62
A_2	2.51	2.51	2.62	2.62
ω_{osc} (rad/sec)	1.010	1.008	1.010	1.011
$\Delta\phi$	90.1^o	90^o	90.0^o	90.0^o

Table 1: Comparing operating point values as computed by solving (27) with the values extracted from Spice-like simulations. Computations were done for $\epsilon = 0.1$.

Besides the characteristics of the resonance tank, there are three other important parameters specifying the design of the oscillator in Fig. 4. So different values of these parameters correspond to different designs. Firstly, we have

$$\gamma = \frac{1/R_{loss}}{g_{m,1}/2} \quad (36)$$

being the ratio between the parallel conductance $G_{loss} = 1/R_{loss}$, modeling capacitor and inductor losses, and the transconductance of the restoring active element (as seen by the resonant tank). Here, g_{m1} is the transconductance of the transistor M_1. A second design parameter is given by

$$m = \frac{g_{m2}}{g_{m1}} \quad (37)$$

which is the ratio of the transconductances of the transistors M_1 and M_2. It is a measure for the strength with which the two oscillators are coupled. Finally, there is ϵ, the ratio between the maximum current which can be delivered by the active elements and the current circulating in the tank. It roughly equals

$$\epsilon = \frac{K}{\gamma Q} \quad (38)$$

where Q equals the quality factor of the inductor coil and where K can be shown to be a constant in the range $0.25 - 1$. This makes ϵ of the same order of magnitude as $1/Q$. For typical Q-factors and choices of γ, ϵ is in the range $0.05 - 0.2$. In what follows, we perform most computations for $\epsilon = 0.1$.

In a first stage, we solve equation (27) for the operating point $\mathbf{q}_{1,op} = \begin{bmatrix} A_1 & A_2 & \Delta\phi \end{bmatrix}$ and $\omega_{osc} = \omega_0 + \Delta\omega_0$. These results are compared with those extracted from SPICE-like simulations. Table 1 summarizes the results for two sets of values for γ and m. All operating point values were found to be at least 1% accurate. This even holds for larger values of ϵ (up to 0.2).

In a next step, we compare the model's transient behavior, in the neighbourhood of the selected operating point, with results obtained from SPICE-like simulations. This is done by starting simulations with initial conditions for amplitudes and phase-differences deviating about 10% from their steady-state values. Fig. 6 shows the resulting amplitudes of the in-phase and quadrature oscillations as computed using the behavioral model (solid line) and as extracted from the envelope of the SPICE-like simulations (x-marks). In order to evaluate the accuracy of the transient model, we computed the ratio of the energy contained in the error component, i.e. the difference between the result obtained from the behavioral model and from the SPICE-like simulations, and the energy contained in the transient itself. The accuracy was computed for two

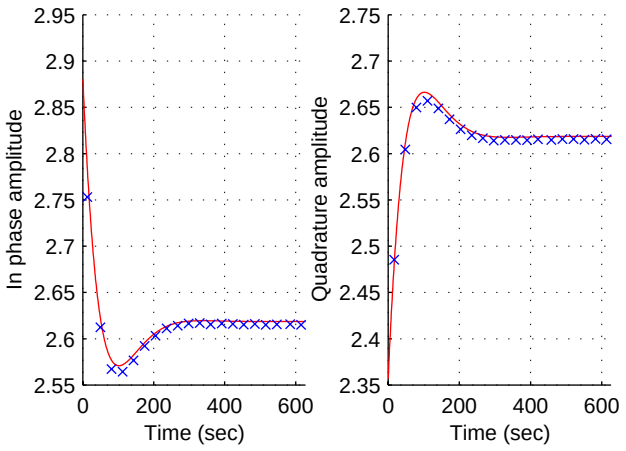

Figure 6: Amplitudes of the in-phase and quadrature oscillations as computed using the behavioral model (solid line) and as extracted from the envelope of the SPICE-like simulations (x-marks). These result were obtained for $\epsilon = 0.1$, $\gamma = 0.5$ and $m = 0.5$.

	Relative error (dB) $\gamma = 0.5, m = 0.3$	Relative error (dB) $\gamma = 0.5, m = 0.5$
$\epsilon = 0.05$	-22.5	-22.1
$\epsilon = 0.1$	-21.9	-20.4
$\epsilon = 0.15$	-18.4	-19.3
$\epsilon = 0.2$	-18.7	-16.4

Table 2: Ratio of the energy contained in the error component, i.e. the difference between the result obtained from the behavioral model and from the SPICE-like simulations, and the energy contained in the transient itself.

sets of values for γ and m and for several values of ϵ, i.e. for several values of the Q-factor of the tank. These results are summarized in Table 2, which shows that, even for larger values of ϵ, the modeling accuracy is still within 1%.

Table 3 compares the computational complexity involved in the evaluation of the original oscillator equations and the behavioral model equations. Both sets of equations were solved with a SPICE-like solver with variable time step. Results are shown for the two extreme values of the parameter ϵ and indicate a speed gain per oscillation period T ranging from 20-40. As expected, speed gain increases with decreasing ϵ due to the larger timestep that can be used in integrating the behavioral model equations. Note that this gain in simulation speed will even further increase when compared to circuit simulations involving more complex transistor models than the level-1 models used in our Matlab experiments. This is due to an increase in computational cost in evaluating the original circuit equations, while the cost in evaluating the behavioral model remains unchanged once it has been computed.

	$\epsilon = 0.05$		$\epsilon = 0.2$	
	Original	Model	Original	Model
CPU-time/T (sec)	0.18	4e-3	0.17	8e-3
KFlops/T	42.5	1.60	42.8	1.93

Table 3: Computational complexity per oscillation period for 2 extreme values of ϵ.

8. CONCLUSIONS

This paper has presented a novel approach for the construction of behavioral models for (coupled) harmonic oscillators. The models can be used for system-level simulations and trade-off analysis. Besides the steady-state behavior, the model also takes transient behavior into account. The modeling equations are valid in the neighbourhood of the oscillator's steady-state operating point. Once being constructed, they can be evaluated at very low computational cost. A major advantage of the approach is that the fast-varying, steady-state, behavior and the slow-varying, transient, behavior are explicitely separated. This allows for straightforward application of multi-rate simulation techniques, boosting simulation speeds with a factor 20 and more. The modeling approach has been applied to a harmonic quadrature oscillator. Results, both as steady state and transient behavior are concerned, were shown to be accurate within 1% as compared to SPICE-like simulations.

9. ACKNOWLEDGEMENTS

This work has been supported in part by the Flemish IWT.

10. REFERENCES

[1] N.N. Bogoliubov and Y.A. Mitropolsky, *Asymptotic methods in the theory of non-linear oscillations*, Hindustan Pulishing Corp., Delhi, 1961

[2] J. Crols and M. Steyaert, *CMOS Wireless Transceiver*, Kluwer Academic Publishers, June 1997

[3] A. Demir et al., "Behavioral Simulation Techniques for Phase/Delay-Locked Systems", In *Proc. IEEE CICC*, pp. 21.3.1-4, 1994

[4] A. Demir, A. Mehrotra and J. Roychowdhury, "Phase Noise in Oscillators: A Unifying Theory and Numerical Methods for Characterization", In *IEEE Trans. Circ. and Syst.-I*, vol. 47, no. 5, pp. 655-674, May 2000

[5] M.I. Freidlin and A.D. Wentzell, *Random perturbations of dynamical systems*, 2nd ed., Springer, 1998

[6] A. Hadjimiri and T.H. Lee, "A General Theory of Phase Noise in Electrical Oscillators", In *IEEE J. Solid-State Circuits*, vol. 33, no. 2, pp. 179-194, February 1998

[7] F.X. Kaertner, "Analysis of White and $f^{-\alpha}$ Noise in Oscillators", In *Int. J. Circuit Theory Appl.*, vol. 18, pp 485-519, 1990

[8] J. Kevorkian and J.D. Cole, *Perturbation Methods in Applied Mathematics*, Springer-Verlag, New York, 1981

[9] N. Kryloff and N. Bogoliubov, *Introduction to non-linear mechanics, Princeton University Press*, New York, 1947

[10] M.F. Mar, "An Event-Driven PLL Behavioral Model with Applications to Design Driven Noise Modeling", In *Proc. BMAS*, Session 1.1, 1999

[11] O. Narayan and J. Roychowdhury, "Multi-Time Simulation of Voltage-Controlled Oscillators", In *Proc. IEEE DAC*, Session 36, 1999

[12] M. Steyaert et al., "A 2-V CMOS Cellular Transceiver Front-End", In *IEEE Journ. Solid-State Circ.*, vol. 35, no. 12, pp. 1895-1907, December 2000

[13] F. Verhulst, *Nonlinear Differential Equations and Dynamical Systems*, 2nd ed., Springer 1996